Food and Chemical Toxicology 69 (2014) 150–162

Contents lists available at ScienceDirect

Food and Chemical Toxicology

journal homepage: www.elsevier.com/locate/foodchemtox

Antrodia cinnamomea profoundly exalted the reversion of activated hepatic stellate cells by the alteration of cellular proteins

Yi-Ren Chen [a], Kai-Ting Chang [a], May-Jywan Tsai [b], Chia-Hung Lee [a], Kao-Jean Huang [a], Henrich Cheng [b], Yen-Peng Ho [c], Jian-Chyi Chen [d], Hsueh-Hui Yang [e], Ching-Feng Weng [a,*]

[a] *Institute of Biotechnology, National Dong Hwa University, Hualien 974, Taiwan*
[b] *Neural Regeneration Laboratory, Neurological Institute, Taipei Veterans General Hospital, Taipei 112, Taiwan*
[c] *Department of Chemistry, National Dong Hwa University, Hualien 974, Taiwan*
[d] *Department of Biotechnology, Southern Taiwan University, Tainan 710, Taiwan*
[e] *Department of Research, Buddhist Tzu Chi General Hospital, General Education Center, Tzu Chi College of Technology, Hualien 970, Taiwan*

ARTICLE INFO

Article history:
Received 14 October 2013
Accepted 4 April 2014
Available online 18 April 2014

Keywords:
Hepatic stellate cells
Proteomic analysis
Reversion
Antrodia cinnamomea

ABSTRACT

The direct modulation of *Antrodia cinnamomea* (AC) on the prominent role of liver fibrosis-hepatic stellate cells (HSCs) *in situ* remains unclear. Firstly, the administration of *A. cinnamomea* mycelial extract (ACME) could improve liver morphology and histological changes including collagen formation and GPT activity in the liver of thioacetamide (TAA)-injured rats. The morphology and fatty acid restore of TAA-induced HSCs (THSCs) returned to the non-chemical induced HSCs (NHSCs) type as measured by immunofluorescence and Oil Red O staining. PPARγ was upregulated associated with the lowering of α-SMA protein in NHSC-ACME. ACME inhibited the MMP-2 activity in NHSCs by gelatin Zymography. After LC–MS/MS, the cytoskeleton (tubulin, lamin A) and heat shock protein 8 in NHSC-ACME, and guanylate kinase, brain-specific kinase, SG-II and p55 proteins were downregulated in THSC-ACME. Whereas MHC class II, SMC6 protein, and phospholipase D were upregulated in NHSC-ACME. Furthermore, PKG-1 was downregulated in NHSC-ACME and upregulated in THSC-ACME. SG-II and p55 proteins were downregulated in NHSC-ACME and THSC-ACME by Western blotting. Taken together, the beneficial effect of *A. cinnamomea* on the induction of HSC cellular proteins is potentially applied as an alternative and complementary medicine for the prevention and amelioration of a liver injury.

1. Introduction

Hepatic stellate cells (HSCs) are one type of non-parenchymal liver cells that reside in the space of Disse. HSCs have the potential to mediate sinusoidal blood flow via contraction, because they release pro-inflammatory, and pro-fibrogenic cytokines (Friedman et al., 1985; Maher, 2001) as well as the intricate factors in the liver microenvironment. In a normal liver, HSCs exist in a quiescent state (qHSCs) that exhibit functions such as vitamin A and retinoid storage as well as reduced extracellular matrix (ECM) formation. HSCs lose their fat storage (mainly retinol) during activation. It remains controversial whether this loss promotes HSC activation and liver fibrogenesis (Kluwe et al., 2011; Lee et al., 2010). During liver injury, qHSCs are trans-differentiated into the activated HSCs (aHSCs), which are also known as myofibroblast-like cells. *In vitro*, HSCs from chronic rat liver-injuries generated by bile-duct ligations are activated as the phagocytes that engulf the hepatocytic apoptosis bodies (Canbay et al., 2002; Torok et al., 2005). Further, NF-κB signaling is remarkably involved in reactive oxygen species (ROS)-induced matrix metalloproteinase 2 (MMP-2) expressions in HSCs (Li et al., 2011). The identification of medicinal fungus that can be used as a complementary and alternative medicine for the protection and/or remedy liver injuries is of significant medical interest.

Antrodia cinnamomea (syn. *Antrodia camphorata*; *Taiwanofungus camphorata*, family Polyporaceae, Aphyllophorales), well known as

Abbreviations: ACME, *Antrodia cinnamomea* mycelial extracts; aHSCs, activated hepatic stellate cells; DAPI, 4′,6-diamidino-2-phenylindole; DMEM, Dulbecco's Modified Eagle's Medium; FBS, fetal bovine serum; LC, liquid chromatography; MS, mass spectrometry; MMP-2, matrix metalloproteinase 2; MTS, (3-(4,5-dimethylthiazol-z-yl)-5(3-carboxymethoxyphenyl)-2-(4-sulfophenyl)-2H-tetrazolium); p55, Tumor Necrosis Factor Receptor 1; PKG-1, cyclic GMP-dependent kinasea-1; PMS, phenazine methosulfate; PPAR-γ, peroxisome proliferator-activated receptor gamma; qHSCs, quiescent hepatic stellate cells; ROS, reactive oxygen species; SG-II, secretogranin II; α-SMA, alpha smooth muscle actin; SMC6, structural maintenance of chromosomes; TAA, thioacetamide.

* Corresponding author. Tel.: +886 3 863 3637; fax: +886 3 863 0255.
E-mail address: cfweng@mail.ndhu.edu.tw (C.-F. Weng).

http://dx.doi.org/10.1016/j.fct.2014.04.006
0278-6915/

niu-chang-chih or jang-jy (Chen et al., 2007; Liau et al., 2007), is a parasitic fungus found in the inner heartwood wall of *Cinnamomum kanehirai* Hay (Lauraceae), which is an endemic species in Taiwan. Three types of bioactive metabolites isolated from (1) fruiting bodies, (2) pure cultured mycelia, and (3) cultured filtrate (cultured broth) are taken as folk medicines or functional foods (Lull et al., 2005). They can be further purified as components for medicines in the near future. The fruiting body of *A. cinnamomea* has been used for many years in folk medicine to treat various diseases and has several biological functions proven in literature review (Geethangili and Tzeng, 2011), such as anti-oxidants (Hseu et al., 2007; Song and Yen, 2002), anti-cancer (Lee et al., 2012), reduce hepatic toxicity (Hsiao et al., 2003; Song and Yen, 2003), anti-viral activities (Lee et al., 2002), anti-inflammation (Shen et al., 2004a), and antibiotic properties (Chen et al., 1995). Nevertheless, the fruiting body of *A. cinnamomea* is naturally rare and expensive when compared with pure cultured mycelia and cultured filtrate. The major chemical components of *A. cinnamomea* have been identified as triterpenoids (Liu et al., 2007a), steroids (Chen et al., 1995), polysaccharides (Lee et al., 2002), and sesquiterpene lactones (Chiang et al., 1995). Recently, expression sequence tags (ESTs) have been used to search for the physiologically active components from *A. cinnamomea* that might be appropriate for the medicinal use (Chen et al., 2007; Wen et al., 2007). CCl_4-induced hepatic toxicity and liver fibrosis in rat models are both reduced by treatment with an extract from a solid-state *A. cinnamomea* mycelial culture (Hsiao et al., 2003; Song and Yen, 2003; Liu et al., 2007b). The methanol extracts from *A. cinnamomea* mycelia possess anti-inflammatory and anti-oxidative properties in *in vitro* and *in vivo* studies (Wen et al., 2011). Moreover, the triterpenoids are major active compounds in the methanol extracts of solid-state cultured *A. cinnamomea* that perform anti-inflammatory activities of microglia *in vivo* and *in vitro* (Liu et al., 2007a). However, the underlying mechanisms for the hepato-protective function of *A. cinnamomea* mycelia from solid culture used to treat chronic liver diseases (i.e., liver fibrosis and cirrhosis), particularly at the cellular levels, remain unclear. This study tested whether *A. cinnamomea* mycelial extracts (ACME) from solid culture could convert an activated state of HSCs into a quiescent state. First, an *in vivo* study was employed to determine the efficacy of ACME on the thioacetamide (TAA)-injured liver of rats. Subsequent non-chemical induced HSC (NHSC) and TAA-induced HSC (THSC) were treated with ACME to find out the efficacy of HSC recovery. The proteomic approach was further performed to investigate the altered profile of cellular proteins in HSCs after treatment.

2. Materials and methods

2.1. Preparation of A. cinnamomea

Air-dried *A. cinnamomea* mycelia grown in solid culture were provided by Comeyoung (Tainan, Taiwan). A total of 100 mg of mycelium with 1 mL ddH_2O was autoclaved at 121 °C for 15 min. After centrifugation, the supernatant was dried up and the solid of ACME was determined around 56 mg/mL. The aqueous *A. cinnamomea* mycelial extract (ACME) was stored at 4 °C before use.

2.1.1. Sugars determination

200 μL of ACME and standards (1–60 μg glucose in 200 μL) were mixed with 200 μL of phenol dissolved in water (5% w/v). 1.0 mL of concentrated sulfuric acid was rapidly and directly added into the solution surface without touching the sides of the tube and kept undisturbed for 10 min before shaking vigorously. The absorbance at 490 nm after additional 30 min reaction was measured to determine the sugars content.

2.1.2. Triterpenoids determination

10 g of ACM powder was extracted in 100 mL 95% alcohol at RT shaking for 12 h and then filtrated out the pellet. The extracts were dried with a vacuum control rotary evaporator (EYELA, Japan). Next, 10 mg extract was dissolved in 10 mL ethyl acetate as a test sample. Accurately 1 mg ursolic acid was dissolved in 10 mL ethyl acetate as a stock standard solution. ACM powder sample and 0–1.20 mL control solution were mixed and dried at 100 °C in water bath. Then 0.40 mL of 5% vanillin–acetic acid solution and 1 mL perchloric acid were added at 60 °C water bath heating for 15 min. The test tube was moved into ice water bath, 5 mL of acetic acid was added, and placed at RT for 15 min. The absorbance was measured at 548.1 nm to determine the total triterpenoids (Lu et al., 2012).

2.1.3. Chromatographic conditions

The HPLC equipment consisted of Waters (Manasquan, New Jersey, USA) pump 626 and Waters 2410 Refractive Index Detector (Manasquan, New Jersey, USA). A Waters Column Oven with Temperature Control Module was used to keep the column temperature constant at 40 ± 0.5 °C. Separation was carried out on a TSK-GEL G5000PWXL column (30 cm × 7.8 mm L × I.D., Tosoh, Japan). 20 μL of ACME solution was introduced into the HPLC system by Waters 717 Autosampler. The flow rate of mobile phase was 0.7 mL/min and consisted of distilled water. Difference molecular weights of dextran (Sigma) were used as standard markers.

2.2. In vivo experiment

Animal experiments were approved by the National Dong-Hwa University Animal Ethics Committee and were used according to the "Guide for the Care and Use of Laboratory Animals" of National Dong-Hwa University. Sprague–Dawley rats (6 weeks old) were purchased from the National Laboratory Animal Center (Taipei, Taiwan) and kept at controlled environmental conditions at room temperature (22 ± 2 °C) and humidity (50 ± 10%). The 12 h light (0600–1800 h) and dark cycle was maintained throughout the study. Rats had free access to food and water and maintained on a standard laboratory diet (carbohydrates; 30%, proteins; 22%, lipids; 12%, vitamins; 3%) ad libitum. Sprague–Dawley rats were injected with thioacetamide (TAA, 200 mg/kg Bwt/3 days, ip) for 30 days to induce liver injury. Afterward, liver-injured rats were orally administrated three times with ACME (1 g/kg Bwt/day) in 10 days. The morphology of livers was examined and recorded. One part of the liver was sampled for histological examinations (hematoxylin and eosin, H and E) stain, Sirius red stain for collagen, and quantification was used as ImageJ software, http://imagej.nih.gov/). The levels of GOT and GPT in the blood serum, as a hepatic index for determining the status of liver function, were measured using the Johnson & Johnson assay in the Vitros 750 (Johnson & Johnson Clinical Diagnostics, Rochester, NY, USA), a kinetic enzymatic assay in which the rate of formation of the final oxidized leuco dye is monitored at 670 nm. All assays were performed according to the protocol described by the manufacturers.

2.3. Cell cultures and viability assay

Preparation of NHSCs and THSCs from livers of male Sprague–Dawley rats (350–400 g, National Laboratory's Animal Center, Taipei, Taiwan) were performed as previously described (Chang et al., 2009). Briefly, THSC was isolated from thioacetamide-induced (TAA, Fluka, Buchs, Switzerland) liver fibrotic rats (also refer to *in vivo* experiment). NHSC represented non-chemical induced HSC and was originally isolated from naive rats. After culture, NHSCs also became the activated form of HSC. The properties of THSCs and NHSCs have been characterized from fibrotic markers in our previous study (Chang et al., 2009), to suggest that THSCs are more active than NHSCs. Two types of HSCs including THSCs and NHSCs were used in this study. Both cell lines were grown and maintained in Dulbecco's Modified Eagle's Medium (DMEM; GIBCO, Carlsbad, CA, USA) containing 10% fetal bovine serum (FBS, GIBCO) (v/v) in an incubator with a humidified atmosphere containing 5% CO_2 at 37 °C. A total of 3×10^4 NHSC and THSC cells were grown separately in 96-well plates for 20 h and were treated with various concentrations (0–10 mg/mL) of ACME for 24, 48, and 72 h. Reagent for cell viability assay was prepared by mixing 2 mL of 2 mg/mL MTS (3-(4,5-dimethylthiazol-z-yl)-5(3-carboxy methoxyphenyl)-2-(4-sulfophenyl)-2H- tetrazolium) (Promega, Madison, WI, USA) with 100 μL of 0.92 mg/mL phenazine methosulfate (PMS, Sigma). A total of 20 μL of MTS/PMS solution was added to each well of ACME-treated NHSC or THSC cells, and the cells were incubated for 1 h at 37 °C in a humidified 5% CO_2 atmosphere. The absorbance was measured at 490 nm using an ELISA plate reader (Thermo LabSystems, Opsys MR, Thermo Fisher Scientific, Waltham, MA, USA).

2.4. Oil red O staining

NHSC and THSC cells (3×10^4) were grown in 6-well or 12-well plates for 24 h prior to use. The cells were treated with 1.25 mg/mL of ACME for additional 24 h. ACME-treated or untreated cells were washed twice with PBS (50 mM sodium phosphate pH 7.4, 0.15 M NaCl) and were fixed with 4% paraformaldehyde for 15 min. An Oil red O working solution was prepared by adding 6 mL of stock solution (0.5 g Oil red O in 100 mL isopropanol) to 4 mL of ddH_2O, then vortex mixing and filtering through a 0.22 μm filter. The fixation agent was removed, Oil red O was added and incubated for 1 h at room temperature (RT) in a dark box. The Oil red O was removed and the cells were washed twice with distilled water. Nuclei were stained with hematoxylin for bright-field microscopic examination and used ImageJ software for quantification. The NHSC and THSC slides were stored in glycerol.

2.5. Immunofluorescence microscopy

NHSCs and THSCs (3×10^4 cells) were cultured on glass coverslips for 24 h and treated with or without ACME for additional 24 h. The cells were washed twice in PBS and were fixed with 4% paraformaldehyde for 15 min. After the PBS wash, the cells were permeabilized with 0.5% of Triton X-100 in PBS for 5 min. The cells were again washed with PBS and were incubated with 200 μL of 100 nM rhodamine phalloidin (F-actin) (Cytoskeleton, Cytoskeleton, Denver, CO, USA) for 30 min in the dark. Subsequently, the cells were washed thrice with PBS. The glass coverslip was fixed on the slide and examined under a fluorescence microscope (OLYMPUS U-RFLT50, OLYMPUS, Tokyo, Japan) equipped with a digital CCD camera (SPOT, Diagnostic Instruments Inc., Sterling Heights, MI, USA). Again, NHSCs and THSCs (3×10^4 cells) were cultured on glass coverslips for 24 h before treatment with or without ACME for additional 24 h. Cells were washed twice with PBS (50 mM sodium phosphate pH 7.4, 0.15 M NaCl) and were fixed with 4% paraformaldehyde for 15 min. Subsequently, the cells were washed with PBS for 5 min and were then blocked with 2% BSA (Sigma) for 1 h. The first antibody (alpha smooth muscle actin, α-SMA; Abcam, UK) was then added, and the cells were incubated at 4 °C overnight. After the overnight incubation, the cells were washed thrice with PBS for 5 min, the second antibody was added (Donkey anti-rabbit Cy3, Jackson ImmunoResearch Laboratories, Inc., West Grove, PA, USA) to each well, and the cells were incubated in the dark at RT for 1 h. The cells were then washed with PBS for 5 min and incubated for 5 min with 300 nM of DAPI (4′,6-diamidino-2-phenylindole, Molecular Probes™, Invitrogen, Eugene, OR, USA). The DAPI was removed and the cells were washed twice with PBS. The specimens were then examined using fluorescence microscopy and used Image J software for quantification.

2.6. Zymography assay for MMP-2 activity

A total of 2×10^5 NHSC and THSC cells were seeded in 6-well plates and grown for 24 h in DMEM medium with 10% FBS. The media were replaced with serum-free DMEM containing 0.1% BSA medium and cells were treated with or without ACME. After 24 h of incubation, media were collected, and protein concentrations were determined. Total protein for each sample (6 μg) was fractionated on 8% SDS-polyacrylamide gel containing 0.1% gelatin. Separated gels were washed twice with washing buffer (2.5% w/v Triton-X-100) at RT for 30 min, then incubated in development buffer (0.02% NaN_3, 0.05 M Tris–HCl pH 8.8, 5 mM $CaCl_2$) for 12 h at 37 °C, and lastly washed twice with fixing/destaining solution (45% methanol, 10% acetic acid, 45% water). The gel was then stained with 0.5% Coomassie Brilliant Blue R-250 (w/v) in fixing/destaining solution for 30 min and destained the gel with fixing/destaining solution until clear bands appeared. Proteinase activity was detected as unstained bands on blue background representing the areas of gelatin digestion, and the activities of MMP-2 in the gel slabs were quantified using an image analysis program.

2.7. Western blotting

A total of 3×10^5 NHSC and THSC cells treated with or without ACME for 24 h and the cells were homogenized in a homogenization solution (137 mM NaCl, 1 mM $CaCl_2$, 1 mM $MgCl_2$, 0.1 mM sodium ortho-vanadate, 20 mM Tris–HCl pH 6.8, 10 g/L NP-40, and 1 mM PMSF) and were centrifuged at 11,300×*g* for 30 min at 4 °C. The supernatant was then stored at −70 °C. Protein immune-blotting was performed as follows: 30 μg of protein was resolved by SDS-polyacrylamide gel electrophoresis and was transferred to PVDF membranes (NENTM Life Science Products, Boston, MA, USA), and the blot was incubated with monoclonal and polyclonal antibodies (Peroxisome proliferator-activated receptor gamma, PPAR-γ: Novus Biologicals, Littleton, CO, USA; α-SMA: Abcam, UK; Cyclic GMP-dependent kinasea-1, PKG-1: Cell Signaling, Danvers, MA, USA; Secretogranin II, SG-II: Santa Cruz, CA, USA; Tumor Necrosis Factor Receptor 1, p55: United States Biological, Swampscott, MA, USA). Following incubation with horseradish peroxidase-conjugated secondary antibodies for additional 1 h, the signals of proteins were visualized with Western Lightning Chemiluminescence Reagent (PerkinElmer Life Sciences, Boston, MA, USA) after wash.

2.8. Sample preparation for 2D gel electrophoresis

NHSC and THSC cells (3×10^5 of each type) were cultured in medium or treated with ACME after being grown for 24 h at 37 °C in a humidified incubator with 5% CO_2 atmosphere. The cells were washed thrice with PBS and were lysed in lysis buffer (7 M urea, 2 M thiourea, 4% CHAPS, 1 mM EDTA, 100 mM DTT, 20 mL Roche Complete, mini protease inhibitor cocktail per 500 μL buffer; 100 μL buffer per 1×10^6 cells) at RT for 1 h by vortex mixing. The samples were then centrifuged at 60,000×*g* at 15 °C for 2 h in an Optima TLX Tabletop ultracentrifuge (Beckman Coulter, Fullerton, CA, USA). After centrifugation, the supernatant was cleaned with a 2-D clean kit (GE Healthcare Life Sciences, Piscataway, NJ, USA) according to the manufacturer's instructions. The protein pellet was dissolved in rehydration buffer and stored at −80 °C. The protein concentration was determined using a protein assay kit (Bio-Rad, Hercules, CA, USA).

2.9. Two-dimensional electrophoresis

After samples containing 300 μg aliquots of protein were loaded onto pH 4–7, 17 cm IPG strips (Bio-Rad); the strips were subjected to the process of passive rehydration at 20 V for 18 h at 20 °C. Isoelectric focusing (IEF) was performed for a total of 60,000 Vh at 20 °C. The isoelectrically focused strip was stored at −20 °C and used directly for the second-dimension electrophoresis. The strips were first equilibrated with solution I (6 M urea, 20% SDS, 1.5 M Tri–HCl (pH 8.8), 30% glycerol, ddH_2O, and 2% DTT) for 15 min, and the strips were then equilibrated with solution II (6 M urea, 20% SDS, 1.5 M Tris–HCl (pH 8.8), 30% glycerol, ddH_2O, and 2.5% iodoacetamide) for 15 min prior to second-dimension SDS-PAGE. The proteins were separated using 10% SDS-PAGE (18 cm × 18 cm × 1.5 mm). The 2D gels were stained using Silver Nitrate Crystal (Mallinckrodt Chemical, Phillipsburg, NJ, USA). The statistical data (spot detection, spot editing, pattern matching, and up- and down-regulation analysis) were acquired and analyzed using the ImageMaster 2D Elite software package, version 5.01 (Nonlinear Dynamics, Newcastle, UK).

2.10. In-gel digestion

Proteins of interest were manually excised from silver stained gels. The gels were first destained with 25 mM of ammonium bicarbonate for 10 min, and then the solution was discarded. Afterward, the gels were destained with 25 mM ammonium bicarbonate (ABC)/50% acetonitrile for 10 min, and then the solution was discarded. These two steps were repeated three times to remove Sypro Ruby staining followed by drying the gels in a SpeedVac concentrator. The dried gels were swollen in 10 mM DTT/25 mM ABC at 56 °C for 1 h to reduce the proteins. After the solutions were discarded, 55 mM iodoacetamide/25 mM ABC was added to the gels and kept in the dark at RT for 45 min to alkylate the proteins. Upon removal of the liquid phase, the gels were washed with 25 mM ABC, 25 mM ABC/50% acetonitrile and 100% acetonitrile, consecutively. The proteins were digested with 10 μL of sequencing grade trypsin (0.1 mg/mL; Promega) in 25 mM ABC overnight at 37 °C. The resulting peptides were extracted from gel pieces with 5% formic acid/50% acetonitrile by sonication.

2.11. Protein Identification

Digested proteins were analyzed by nanoscale capillary LC–MS/MS using an UltimateTM capillary LC system, Switchos valve switching unit and Famos autosampler (LC Packings, San Francisco, CA, USA) coupled to a quadrupole time-of-flight mass spectrometer (QSTAR XL, Applied Biosystem/MDS Sciex, Foster City, CA, USA) equipped with a nano-spray ionization source. Around 2.5 μL of sample was injected through an auto-sampler into the LC system at the flow rate of 30 μL/min and pre-concentrated on a 300 μm × 5 mm PepMap C18 precolumn (LC Packings). The peptides were then eluted onto a 75 μm × 150 mm NanoEase C18 analytical column (Waters Corp., Milford, MA, USA). The column was equilibrated with solution A (5% ACN, 94.9% water, 0.1% formic acid), and the peptide separation was achieved with a solution gradient from 5% to 60% of solution B (80% ACN, 19.9% water, 0.1% formic acid), over 47 min at a flow rate of 200 nL/min. The flow rate through the column was reduced from 200 nL/min by a flow splitting unit. The LC eluent was directed to the electrospray source with a PicoTip emitter (New Objectives, Woburn, MA, USA). The mass spectrometer was operated in a positive ion mode. TOF analyzer was calibrated with a multi-point calibration using selected fragment ions from the CID of Glu-fibrinopeptide B. MS/MS spectra were obtained in an information-dependent acquisition method (IDA). The MS/MS data were subjected to search algorithms against Swiss-Prot or NCBInr protein sequence database using Mascot software (Matrix Science Ltd., London, UK).

2.12. Statistical analysis

Experimental data are presented as means ± standard deviation (SD). Comparisons of the control samples with the treated samples were analyzed by a one-way ANOVA followed by an LSD *t*-test (SAS 2004). * ($P < 0.05$), ** ($P < 0.01$), and *** ($P < 0.005$) indicate significant differences as compared with the control group.

3. Results

ACM powder contained 107 mg sugar/g and 91.9 mg total triterpenoids/g. Further, SE-HPLC data Analysis, ACME was separated two major peaks. The molecular weights of two major peaks were about 30 kDa and 100 kDa (Supplement Fig. 1).

3.1. Effects of ACME on TAA-injured rats in vivo

An *in vivo* experiment was conducted to check the protective effect of ACME. Ten doses of i.p. injection of TAA to rats induced serious liver damage (Fig. 1A), collagen formation (Fig. 1B), and

concurrently elevated both GOT and GPT levels (Fig. 1C). The administration of ACME could improve the liver morphology (Fig. 1A), histological changes including collagen (Fig. 1D), and GPT in liver of TAA-injured rats (Fig. 1C). This *in vivo* experiment was mainly confirmed the efficacy of ACME on the alleviation of liver fibrosis.

3.2. Cell viability and Fatty acid storage of HSCs treated with ACME

3×10^4 cells (NHSC and THSC) were treated with various concentrations of ACME for 24, 48, and 72 h. The data showed that NHSC (Fig. 2IA) and THSC (Fig. 2IB) cells were treated with 0.18, 0.35, 0.7, 1.4, 2.8, and 5.6 mg/mL of ACME for 24 h. The cell viability of HSC cells was decreased with the concentration of ACME. The cell viability of NHSC cells at various dosages of ACME treatment was more severe than that of THSC cells. This tendency was similar in the treatments no matter different times of treatment. By contrast, HSC cells treated with 2.8 mg/mL of ACME had only a few cells survive. The present study was focused on the reversion of HSCs; hence, low dosages (<1.4 mg/mL) of ACME without causing HSC death were chose for the subsequent experiments. HSC cells (3×10^4) were challenged with 0.18 and 0.7 mg/mL of ACME for 24 h and stained with Oil red O to determine the fat accumulation. NHSC cells treated with 0.7 mg/mL of ACME (NHSC-ACME) could store much more fatty acid than that of untreated NHSC cells (Fig. 2IIA, IIC, and IIE). THSC cells treated with 0.7 mg/mL of ACME (THSC-ACME) were restored little fatty acid as compared with untreated THSC cells (Fig. 2IIB, IID, and IIF). THSC treated with 0.18 and 0.7 mg/mL of ACME were capable of showing fatty acid storage. THSC cells treated with 0.7 mg/mL of ACME had more fatty acid than that of THSC cells treated with 0.18 mg/mL of ACME. NHSC and THSC cells treated with 0.7 mg/mL of ACME were showed large lipid droplets. According to the amount of fatty acid storage observed, the efficiency of treatments can be ordered as follows: NHSC-ACME > NHSC > THSC-ACME > THSC.

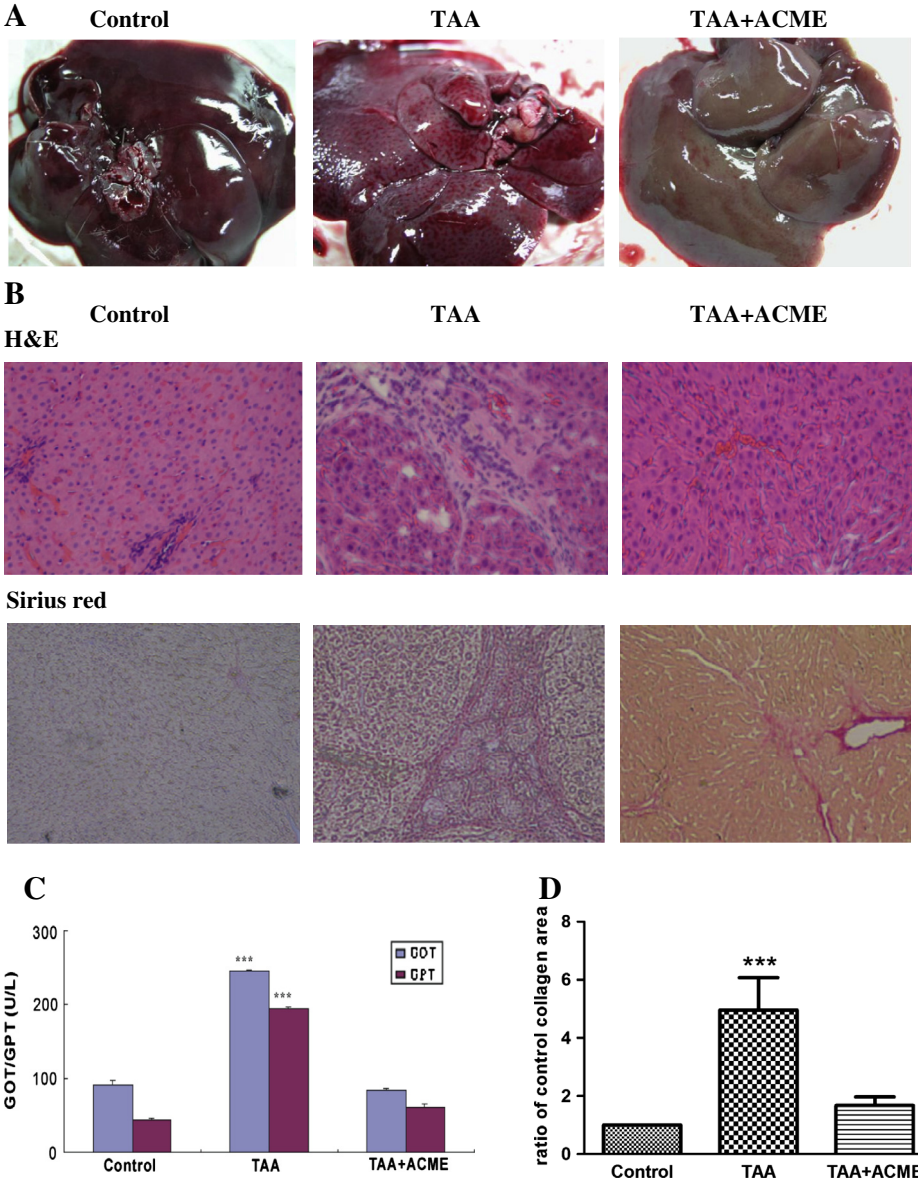

Fig. 1. Liver morphologies (A), histological changes (B), plasma GOT/GPT levels (C), and (D) the protein levels of collagen relative to the control in TAA-injured rats or in TAA-injured rats after aqueous *A. cinnamomea* mycelial extract (ACME) treatment. Sprague–Dawley rats were performed in this assay, each group contained 8 rats. One part of the liver was fixed and dissected for histological examinations (hematoxylin and eosin, H and E) stain, Sirius red stain for collagen). Values for each graph represent the mean ± SD. $^{***}P < 0.001$ presents the level of significant difference in the TAA and TAA + ACME treatments.

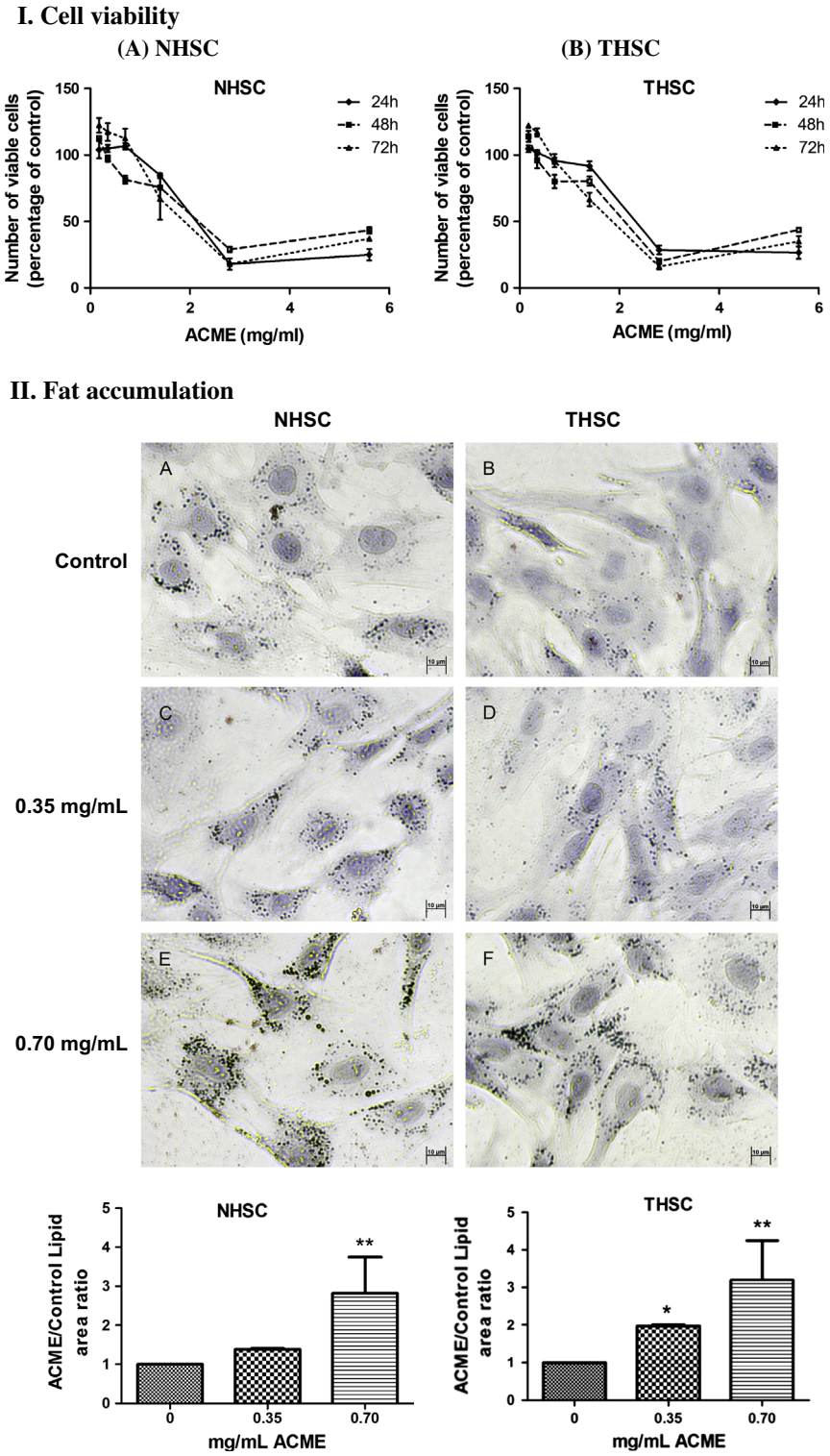

Fig. 2. Cell viability and fat accumulation of NSHCs and THSCs treated with aqueous *A. cinnamomea* mycelial extract (ACME). (I) cell viability was determined at different time courses after ACME treatment in (A) 3×10^4 NHSCs and (B) 3×10^4 THSCs cells by MTS assay; (II) Fat accumulation in NHSCs (A, C, and E) and THSCs (B, D, and F) treated without or with 0.35 and 0.70 mg/mL of ACME for 24 h stained with Oil red O. The independent experiments were repeated three times. $^{*}P < 0.05$ and $^{**}P < 0.01$ presents the level of significant difference in the control and treatment.

3.3. Morphological alteration of HSCs treated with ACME

Neither NHSC nor THSC cells were different from NHSC-ACME and THSC-ACME cells, with respect to the immunofluorescence staining was observed using α-SMA antibodies (Fig. 3I) and F-actin staining (Fig. 3II). No differences in morphology were observed between NHSC-ACME and THSC-ACME cells as assayed by F-actin staining. The data showed that ACME could inhibit the α-SMA protein in NHSCs with a dose-dependent manner but no significant effect on THSCs was found (Fig. 3I).

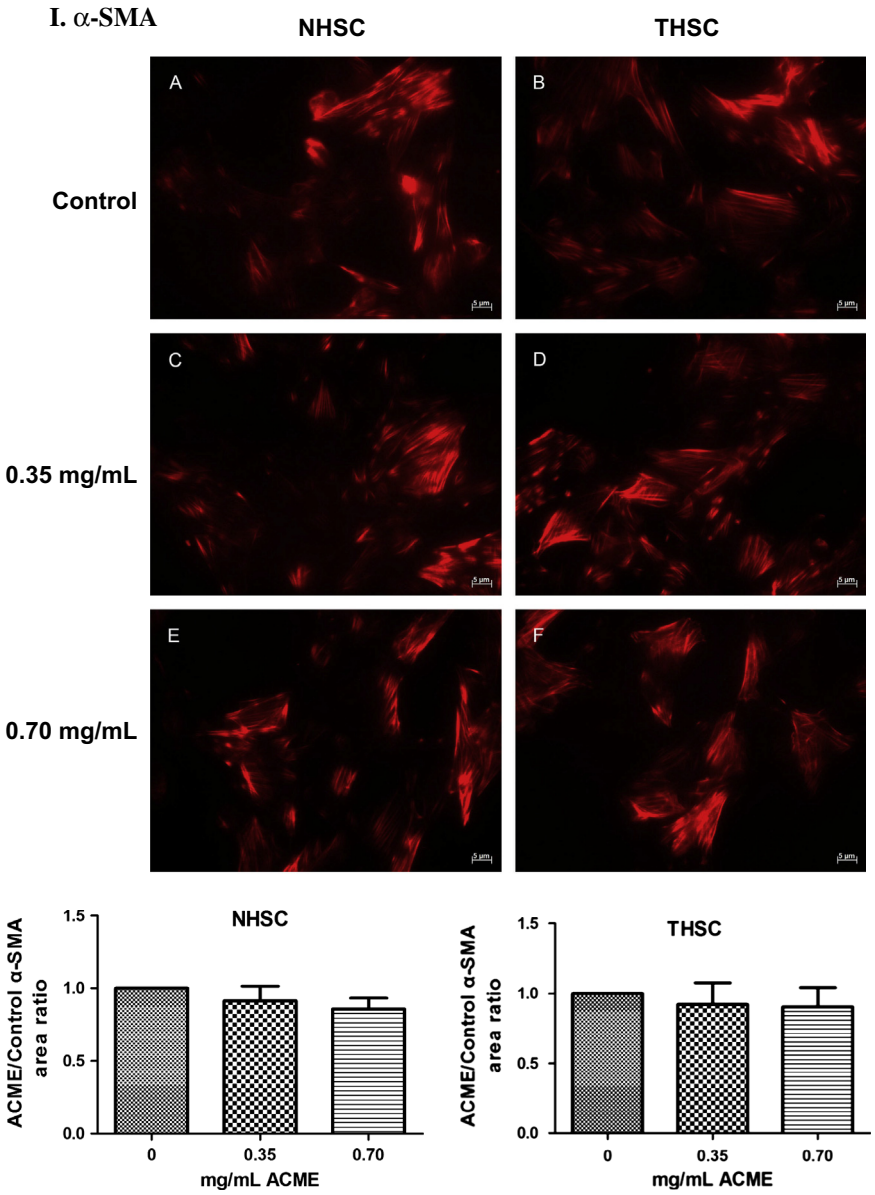

Fig. 3. Morphologies of naïve or aqueous *A. cinnamomea* mycelial extract (ACME)-treated NHSCs and THSCs. Both NHSCs and THSCs were treated with 0.7 mg/mL of aqueous *A. cinnamomea* mycelial extract (ACME) for 24 h stained by immunofluorescence (I) alpha smooth muscle actin (α-SMA) in NHSCs (A, C, and E) and THSCs (B, D, and F) treated without or with 0.35 and 0.70 mg/mL and (II) F-actin with rhodamine phalloidin (A and B) are the control group and (C and D) present the 0.70 mg/mL of ACME treatment group.

3.4. Regulation of PPAR-γ, α-SMA, and MMP-2 expressions in HSCs treated with ACME

Western blot revealed that PPAR-γ and α-SMA were expressed in both NHSC and THSC cells treated or untreated with ACME (Fig. 4A); PPAR-γ protein level was upregulated in NHSC-ACME but no significant effect on THSC-ACME (Fig. 4B). The expression level of α-SMA was downregulated in NHSC-ACME where no significant effect on THSC-ACME was found (Fig. 4C). Gelatin zymography was applied to measure the MMP-2 activity in both HSCs treated with 0.18, 0.35, and 0.7 mg/mL of ACME. The data showed that ACME could inhibit the MMP-2 activity in NHSCs with a dose-dependent manner but no significant effect on THSCs was found (Fig. 5).

3.5. Differential proteins expressed in ACME-treated HSCs

The protein profiles of NHSC versus NHSC-ACME cells were different as measured by 2-D gel electrophoresis (Fig. 6A). There were 24 cellular protein levels varied by more than twofold between NHSC and NHSC-ACME cells; ten proteins showed the increase of expression and 14 proteins showed the decrease of expression. The protein profiles of THSC and THSC-ACME cells were also different when observed using 2-D electrophoresis (Fig. 6B). There were 19 cellular proteins levels changed at least twofold between THSC and THSC-ACME cells; the increased expression of 8 proteins and the decreased expression of 11 proteins were found. Using LC–MS/MS, the proteins were differentially expressed in between NHSC and NHSC-ACME cells including three translocation factors (zfp2, zfp108, and hypothetical zinc finger), two unknown proteins, two kinds of immunoproteins (immunoglobulin like variable motif-containing protein and MHC class II), two cytoskeletal proteins (tubulin and lamin A), a hypothetical protein, SMC6, phospholipase D (PLD), poly(A)-binding protein, heat shock protein 8, and Podn protein (Table 1A). SMC6, PLD, poly(A)-binding protein, and MHC class II antigen beta chain were elevated whereas tubulin, lamin A,

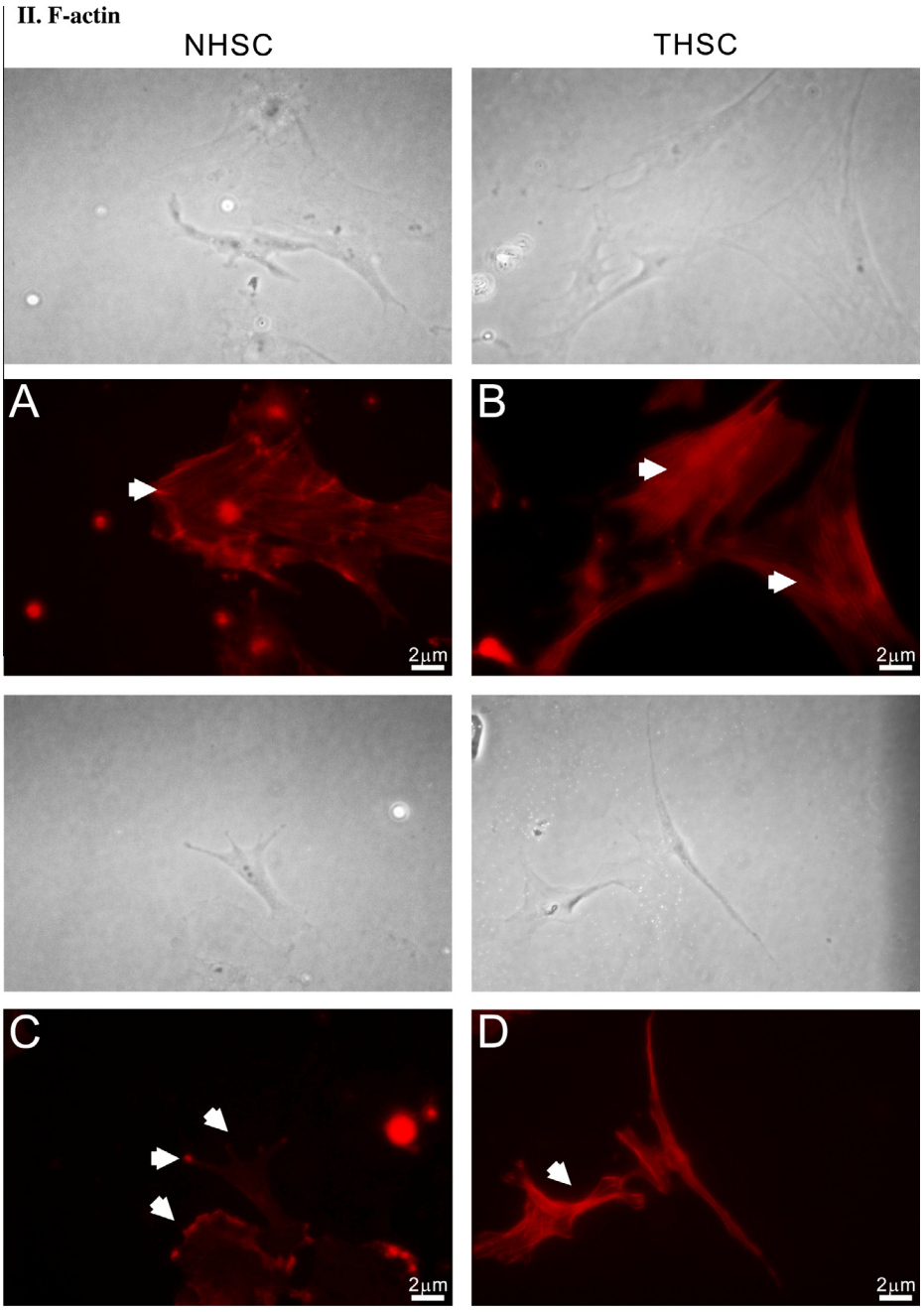

Fig. 3 (*continued*)

heat shock protein 8, and Podn protein were decreased in NHSCs treated with ACME. Additionally, the proteins differentially expressed in between THSC and THSC-ACME cells including six unknown proteins, secretogranin II (SG-II), guanylate kinase (GMP kinase), epididymal-specific lipocalin (ELP16), brain-specific kinase, and p55 protein (Table 1B). ELP16 was upregulated while GMP kinase, SG-II, brain-specific kinase, and p55 protein were downregulated in THSCs treated with ACME. The validation of explored proteins was confirmed by Western blot analysis. The data revealed that PKG-1 protein level was downregulated in NHSC-ACME but upregulated in THSC-ACME cells. SG-II and p55 protein levels were downregulated in both NHSC and THSC cells treated with ACME (Fig. 7).

4. Discussion

The main finding of this study examined the effectiveness of ACME on HSCs *in vitro* and on TAA-induced liver injury *in vivo*. An ethanol extract from solid-state cultured *A. cinnamomea* (the same material used in this study) can inhibit the proliferation of A549 by inducing endoplasmic reticulum stress, but no cytotoxicity was found in MRC-5s (Wu et al., 2006). Notably, our study provides the first evidence that both NHSCs and THSCs (as aHSCs) treated with ACME can restore fatty acid albeit to different extents. NHSCs stored more fatty acid than THSCs. The lipid droplets observed in NHSC-ACME group was denser than the THSC-ACME group. These aHSCs lose their capability of vitamin A storage;

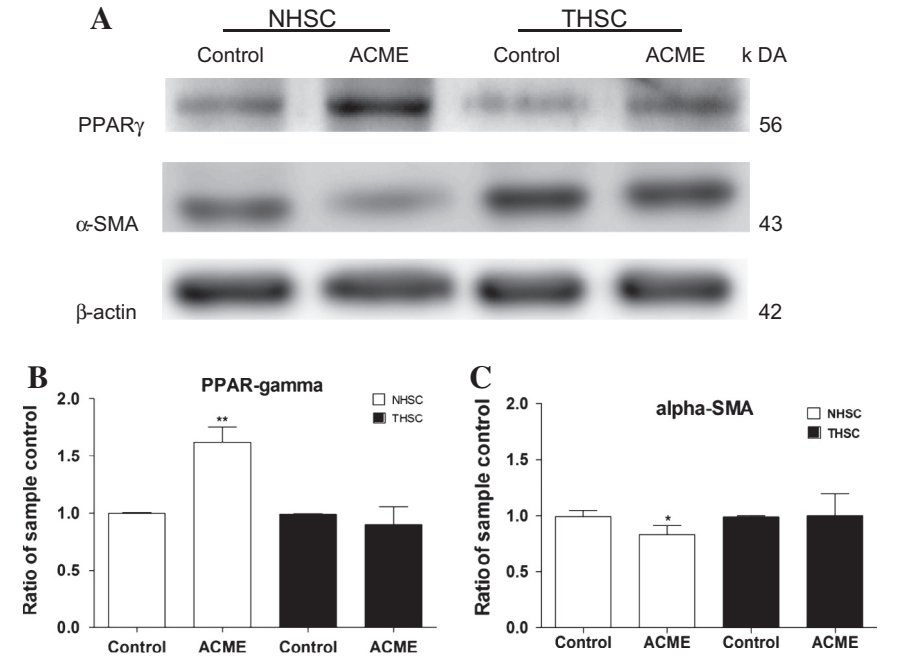

Fig. 4. Expressions of PPAR-γ and α-SMA in NHSCs and THSCs after aqueous *A. cinnamomea* mycelial extract (ACME) treatment. (A) Representative Western blots of cultured HSC homogenates after vehicle or ACME treatment. (B) The protein levels of PPAR-γ relative to the control. (C) The protein levels of α-SMA relative to the control. Cells were untreated or treated with 0.70 mg/mL of ACME for 24 h and processed by Western blot analysis for PPAR-γ and α-SMA using β-actin as an internal control. The independent experiments were repeated three times. $^{*}P < 0.05$, and $^{**}P < 0.01$ present the level of significant difference in the control and treatment.

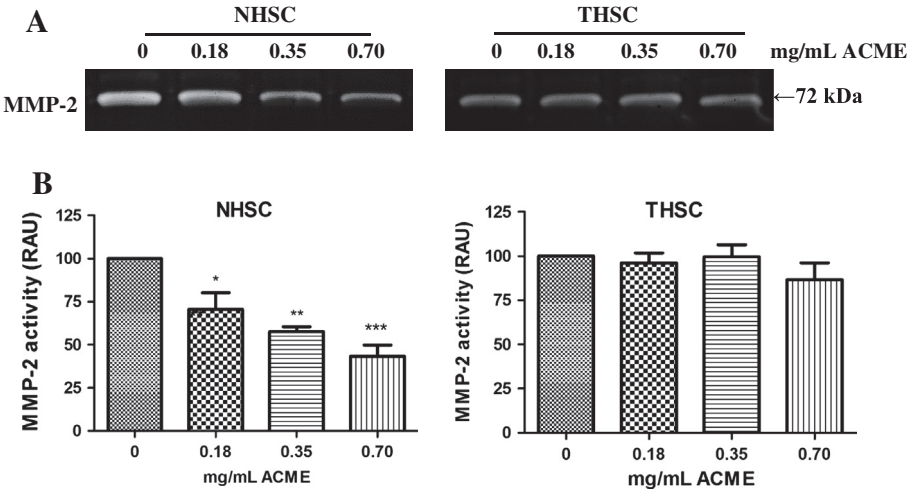

Fig. 5. The activity of matrix metalloproteinase-2 (MMP-2) in naive or aqueous *A. cinnamomea* mycelial extract (ACME)-treated NHSCs and THSCs. (A) Representative gelatin zymography for MMP-2 activity in supernatant of cultured HSC after treatment. (B) The MMP-2 activities in NHSCs and THSCs. Cells were treated with various concentrations (0, 0.18, 0.35, and 0.70 mg/mL) of ACME for 24 h. Gelatin zymography is polyacrylamide gels copolymerized with gelatin (1 mg/mL) employed to measure the enzymatic activity of MMP-2. Values for each graph represent the mean ± SD. RAU, relative absorbance unit. The independent experiments were repeated three times. $^{*}P < 0.05$, $^{**}P < 0.01$, and $^{***}P < 0.001$ present the level of significant difference in the control (0) and treatment.

subsequently overproducing ECM during the proliferation (Elsharkawy et al., 2005; She et al., 2005). This overproduced ECM is stored in hepatic nodes and the space between cells, consequently causing liver fibrosis. Liver fibrosis is reduced by treatment with an ACME from a solid-state culture in a CCl_4-induced rat models (Hsiao et al., 2003; Song and Yen, 2003; Liu et al., 2007b). In these previous reports (i.e. CCl_4-induced liver injury) specially focused on free radical scavenging mechanism that could affect multiple organs to cause animal death. In our work, the cause of TAA in liver injury is highly liver-specific. Compared with CCl_4-induced liver injury, the phenotype of TAA-injured is more representative for liver injury particular in fibrosis. Additionally, Wistar rats are orally administrated 0.04% TAA (oral water) plus ACME (0.25 and 1.25 g/kg Bwt/day) for 12 weeks. The results demonstrate that ACME can alleviate the extent of liver fibrosis in TAA-injured rats by H&E and Masson's trichrome (Lee et al., 2005 unpublished paper). Up to our knowledge, this is the first evidence that solid ferment *A. cinnamomea* was tested in the efficacy of TAA-induced liver injury. TAA is a typical hepatotoxin, which causes liver damage, centrolobular necrosis, liver fibrosis, and further liver cirrhosis in rats with symptoms resembling liver fibrosis and cirrhosis in human (Fan and Weng, 2005; Muller et al., 1998). In this study, the employed advantage of *A. cinnamomea* mycelia noted that AC mycelia are grown on the solid culture and expanded

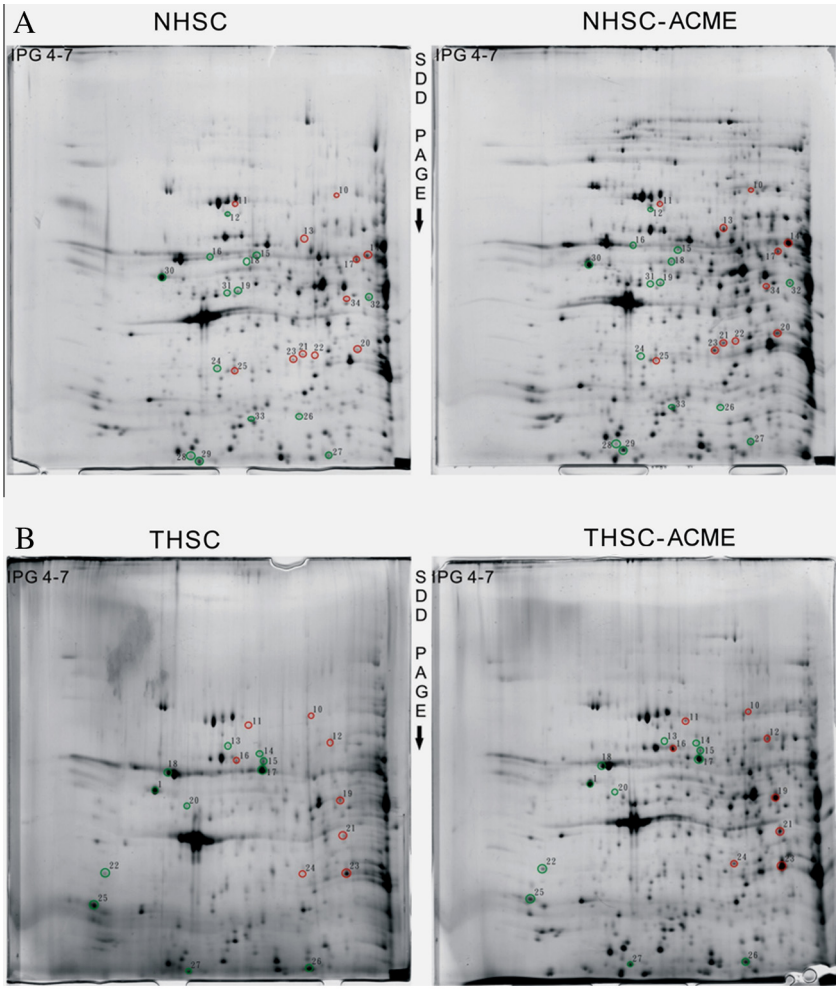

Fig. 6. Comparative protein profiles of (A) NHSC and NHSC-aqueous *A. cinnamomea* mycelial extract and (B) THSC and THSC-ACME. NHSC and THSC were treated with 0.70 mg/mL ACME for 24 h. Moreover, the proteins of cell lysate were isolated and protein patterns were measured by 2-D gel electrophoresis. Red circles represent greater than 2-fold differences between two groups. Green circles represent less than 2-fold differences between two groups.

in large quantity under control. In contrast to the fruiting body of AC that is naturally planted but with a difficult quality control; thereby, the amount is rare and limits its clinical application.

Generally, aHSCs dominantly express desmin, α-SMA (Ramadori et al., 1990), and cytoglobin/stellate cell activation-associated protein (Kawada et al., 2001; Nakatani et al., 2004). For qHSCs may contain either desmin or glial fibrillary acidic protein (GFAP), suggesting that they belong to the smooth muscle cell or glial cell lineages, respectively (Niki et al., 1996). Our previous report has demonstrated that both NHSCs and THSCs can express specific markers for the characteristics of activated cell types (Chang et al., 2009). qHSCs also possess the adipocyte-specific genes including PPAR-γ and sterol-regulatory element binding protein-1 nuclear abundance (nSREBP-1) (She et al., 2005) that regulate the fatty acid storage. PPAR-γ is an adipogenic transcription factor that is expressed in adipose tissue to inhibit the connective tissue growth factor (CTGF) and collagen I (α) expression. Fatty acid storage is regulated by PPAR-γ and this process is inhibited by transforming growth factor beta 1 (TGF-β1); the consequence of PPAR-γ inhibition, HSCs can express the CTGF and pro-collagen I (α) (Fan and Weng, 2005; Sun et al., 2006) resulting in ECM deposit. MMP-2 plays an important role in human liver injury and fibrosis (Arthur et al., 1992). NO/cGMP sensitive store-operated Ca^{2+} entry can cause the MMP production and the adhesion ability of fibroblasts (Huang et al., 2006). The mediation of guanylyl cyclase-coupled natriuretic peptide receptor (NPR)/cGMP/PKG pathway results in the inhibition of collagen production in HSCs and eventually liver fibrosis is ameliorated (Chen et al., 2010). Our results demonstrated that *A. cinnamomea* could inhibit the MMP-2 activity and decrease the expressions of PKG-1 (cGMP) in NHSC cells to avoid cell fibrosis. PPAR-γ agonists (15d-PFJ2, troglitazone, and ciglitazone) can inhibit TGF-β1 expression that decreases the mRNA levels of α-SMA, fibronectin, and collagen III (Wang et al., 2007). In the present study, PPAR-γ protein was elevated in both NHSC-ACME and THSC-ACME cells. Type I collagen (alpha 1 and alpha 2 chains), α-SMA, TGF-β1, TGF-β receptors, platelet-derived growth factor (PDGF), CTGF, MMP-2, and TIMPs 1 & 2 could be used as molecular targets for the index of fibrosis (Lee and Friedman, 2011; Yu et al., 2012). Compared with HSC cells, activated NHSC cells returned to the quiescent state and stored fatty acid again after ACME treatment while the amount of stimulation factor-TGF-β1 is decreased, an increase in the amount of PPAR-γ and a decrease in the amount of α-SMA. But activated THSC cells could not significantly decrease α-SMA, MMP-2 and collagen. In our experimental design was tested in low concentration of ACME and high viability of HSCs to compare with different characteristics among treatments. The highest concentration of ACME (0.75 mg/mL) could not affect the HSCs cell growth and the cell viability was about 90% in 24 h treatment. Review the recent study, caffeine can decrease α-SMA expression in 10 mmol but the cell viability is only 40%. However, caffeine cannot decrease α-SMA expression in 0.1 mmol and the cell

Table 1
Identification of proteins by MASCOT.

Spot number	Expression (compared with NHSC)	Accession number[a]	Protein name	Theoretical pl/Mw (kDa)	Species	Score
(A) NHSC versus NHSC-ACME						
10	Up	Q8R012_MOUSE	Multifinger protein mKr2 (Zfp2 protein)	9.1/52.5	*Mus musculus*	72
17	Up	Q8BLA2_MOUSE	Hypothetical Zinc finger	9.27/67	*Mus musculus*	62
20	Up	Q4V8M1_RAT	Hypothetical protein	9.11/61.2	*Rattus norvegicus*	55
21	Up	AAM45762	Immunoglobulin-like variable motif-containing protein	9.01/56.6	*Mus musculus*	52
22	Up	Q91YZ8_MOUSE	Poly(A) binding protein	9.52/67.8	*Mus musculus*	51
11	Up	Q924W5_MOUSE	SMC6 protein	6.79/127.1	*Mus musculus*	48
14	Up	AAB06393	RNU59245 NID	6.18/161.9	*Rattus norvegicus*	44
23	Up	Q7YQ81_PERCA	MHC class II antigen beta chain	5.33/11.24	*Peromyscus californicus*	39
13	Up	T42093	Phospholipase D	8.84/119.2	*Mus musculus*	38
16	Down	Q6NZD0_MOUSE	Heat shock protein 8	5.28/70.8	*Mus musculus*	71
19	Down	Q9R167_MOUSE	Zinc finger protein ZFP108	8.91/72.9	*Mus musculus*	64
12	Down	AAK56095	AF332067 NID	5.72/120.7	*Mus musculus*	53
24	Down	Q6P3D8_MOUSE	Podn protein	9.69/46.4	*Mus musculus*	52
18	Down	S27267	Lamin A	6.29/74.2	*Rattus norvegicus*	42
15	Down	Q3UIT6_MOUSE	Tubulin	6.37/103.08	*Mus musculus*	40
(B) THSC versus THSC-ACME						
19	Up	Q6KGV4_RAT	Epididymal-specific lipocalin ELP16	7.79/20.6	*Rattus norveg*	72
11	Up	BAA94844	AB033766 NID	4.66/29.2	*Mus musculus*	39
12	Up	AAF05725	AF191551 NID	8.33/89	*Mus musculus*	38
23	Up	AAH05754	BC005754 NID	6.4/33.4	*Mus musculus*	36
25	Down	BAC30363	AK039481 NID	7.9/38.8	*Mus musculus*	63
26	Down	BAA94844	AB033766 NID	4.66/29.2	*Mus musculus*	63
14	Down	I48967	Brain-specific kinase	6.22/97	*Mus musculus*	59
16	Down	S02180	Secretogranin II	4.71/70.98	*Rattus norvegicus*	39
17	Down	KGUA_MOUSE	Guanylate kinase (EC 2.7.4.8) (GMP kinase)	6.14/21.7	*Mus musculus*	40
22	Down	Q6F6B2_RAT	P55 protein	6.01/50.86	*Rattus norvegicus*	38
15	Down	AAF20023	AF155909 NID	5.84/18.61	*Mus musculus*	38

[a] From the database of NCBI.

viability is still 90% (Shim et al., 2013). These results demonstrate that *A. cinnamomea* mycelia from a solid culture may have the capability to restore fatty acid storage in aHSCs that returned to the quiescent state (qHSCs).

The cytoskeleton (tubulin and lamin A) and heat shock protein 8 in NHSC-ACME, and several proteins including guanylate kinase, brain-specific kinase, secretogranin II (SG-II), and p55 proteins in THSC-ACME were downregulated. Lamin A plays an important role in the structure and function of the nucleus affecting nuclear morphology and cell proliferation (Kudlow et al., 2008; Zhang and Sarge, 2008). Our results may be caused by the functions of lamin A including the control of nuclear morphology and decrease of cell proliferation. Secretoneurin derived from SG-II that seems to act as a pro-inflammatory protein, regulating migration, and proliferation of cells involved in inflammatory responses (Kähler et al., 1997). p55-related molecule is implicated in fulminant hepatic injury (Ogasawara et al., 1993; Galle et al., 1995). HSCs have the major interactions that occur in the development of hepatic injury and fibrosis such as crosstalk between parenchymal and non-parenchymal cells (Gressner and Weiskirchen, 2006; Prosser et al., 2006). p55-mediated signals may regulate the activation of Kupffer cells and HSCs to enhance fibrotic process (Kitamura et al., 2002). Additionally, the fruiting body of *A. cinnamomea* is applied as an anti-inflammatory reagent (Shen et al., 2004b), and reduces the hepatic toxicity (Hsiao et al., 2003; Song and Yen, 2003). Both triterpenoid-betulin and betulinic acid have been shown to inhibit HSCs migration as well as the production of TGF-β1 and ethanol-induced tumor necrotic factor (TNF)-α (Szuster-Ciesielska et al., 2011). Therefore, *A. cinnamomea* may dampen the activity of autocrine inflammatory factors such as TNF-α to alleviate inflammation and subsequently restore fatty acid storage. One report indicates that lack of tumor necrosis factor receptor type 1 can inhibit the occurrence of liver fibrosis (Sudo et al., 2005), implying that pro-inflammatory factors fail to interact with its own receptor to trigger inflammation. By downregulated, SG-II protein may dampen the secretoneurin protein expression that can further inhibit the migration of fibroblasts, and the p55 protein may be a pro-inflammatory factor is downregulated to prevent inflammation. Therefore, the inhibition of SG-II and p55 after ACME treatment could cause less inflammation in THSC-ACME. This result infers that *A. cinnamomea* mycelia from solid culture possess beneficial effects for converting HSCs from aHSCs to qHSCs via the reduction of inflammation.

Accordingly MHC class II, SMC6 protein, and PLD in NHSC-ACME; and ELP16 in THSC-ACME were upregulated. PLD has two major isoforms (PLD1 and PLD2) that are particularly relevant to the activation of HSCs. PLD regulates cell contraction/migration and cell proliferation via effects on the cytoskeleton and the activation of ERK (Iyer and Kusner, 1999; Kam and Exton, 2001). *In vivo* study, co-administration with a purified preparation of PLD dramatically increases the onset of fibrosis/cirrhosis in the CCl_4 rat model (Ozeki et al., 1985). In eukaryotes, there are three conserved structural maintenance of chromosome (SMC) complexes that each builds around two SMC proteins (Losada and Hirano, 2005). SMC6 is activated in DNA repair and is for checkpoint signaling (Lehmann et al., 1995; Taylor et al., 2001). Poly(A)-binding protein (PABPN1) is involved in the synthesis of mRNA poly(A) tails in most eukaryotes (Kühn et al., 2003). These results suggest that some HSC cellular proteins might be induced for the alleviation of liver fibrosis by ACME treatment.

In conclusion, with regard to the liver fibrogenic mechanism, ACME from solid culture inhibits the MMP-2 activity, down-regulates the α-SMA and up-regulates the PPAR-γ gene expressions in HSCs *in vitro*. The effect of ACME on the induction of HSC cellular proteins might be involved in the diminution of liver fibrosis. The remarkable inhibition of SG-II and p55 protein in the activation of HCS makes the ACME as a promising agent for potential anti-inflammatory combination therapies. *In vivo* experiment is

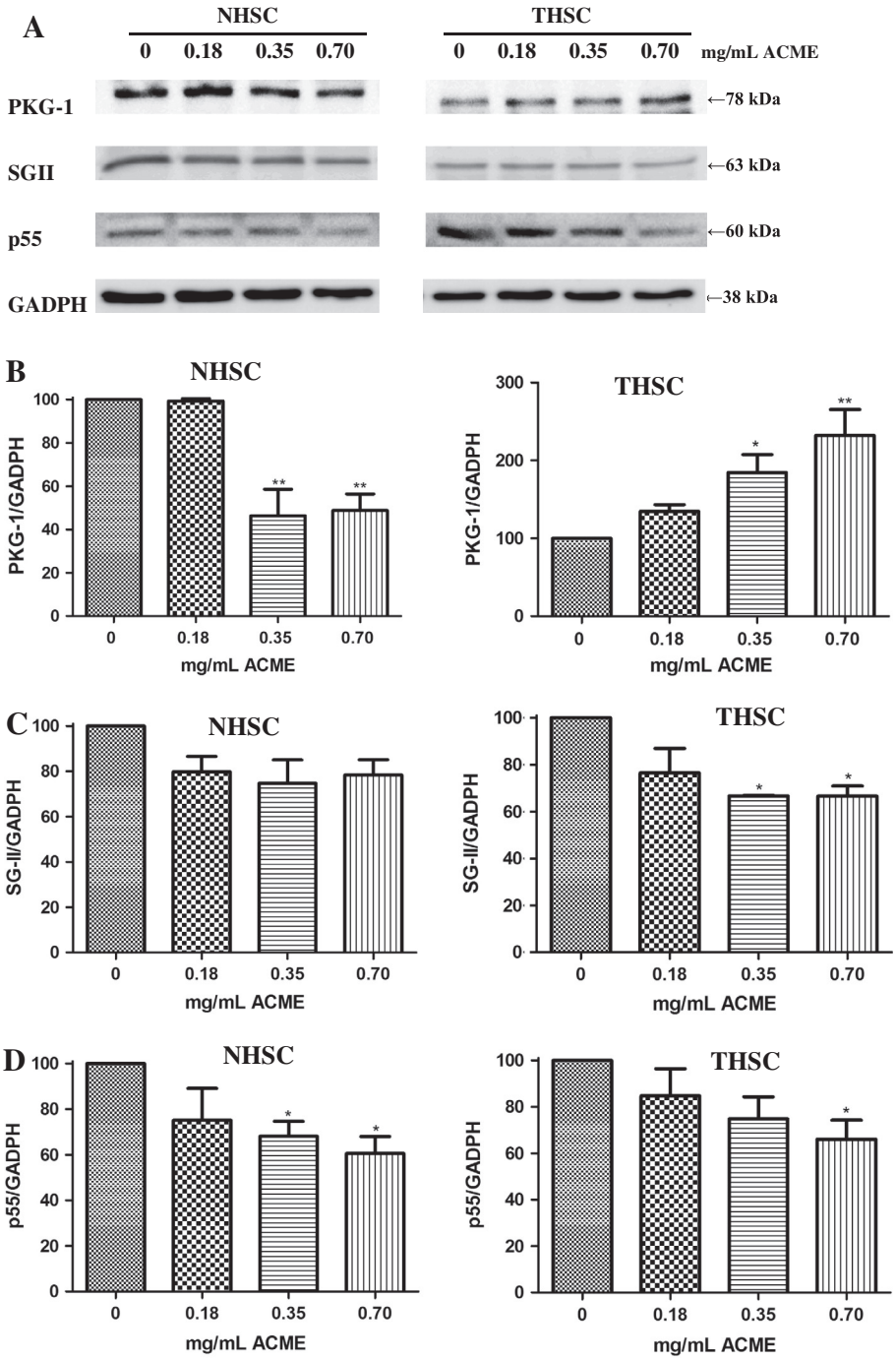

Fig. 7. Effect of aqueous *A. cinnamomea* mycelial extract (ACME) on the protein levels of PKG-1, SG-II, and p55 in NHSC and THSC. (A) Representative Western blots of cultured HSC homogenates after treatment. The protein levels of PKG-1 (B), SG-II (C), and p55 (D) in NHSC and THSC. Cells were treated with various concentrations (0, 0.18, 0.35, and 0.70 mg/mL) of ACME for 24 h and processed by Western blot analysis for PKG-1 (B), SG-II (C), and p55 (D) using GAPDH as an internal control. The independent experiments were repeated three times. $^{*}P < 0.05$ and $^{**}P < 0.01$ present the level of significant difference in the control (0) and treatment.

further confirmed by the efficacy of ACME on the alleviation of liver fibrosis and reduced GOP/GTP inflammatory factor. Taken together, *Antrodia cinnamomea* is applied as an alternative and complementary medicine for the prevention of liver fibrosis via anti-inflammation provides further molecular support from this study.

Conflict of Interest

The authors declare that there are no conflicts of interest.

Transparency Document

The Transparency document associated with this article can be found in the online version.

Acknowledgments

We sincerely thank Miss Yu-Ju Tzeng who helps us to run the Bio-AFM and Professor Je-Wen Liou (Department of Biochemistry,

School of Medicine, Tzu-Chi University, Hualien, Taiwan) who kindly provided the AFM instrument. This study was supported by Grants from the National Science Council (NSC-98-2622-B-259-001-CC3, NSC-98-2218-E-007-004 and NSC-99-2311-B-259-001-MY3) to C.F. Weng.

Appendix A. Supplementary material

Supplementary data associated with this article can be found, in the online version, at http://dx.doi.org/10.1016/j.fct.2014.04.006.

References

Arthur, M.J., Stanley, A., Iredale, J.P., Rafferty, J.A., Hembry, R.M., Friedman, S.L., 1992. Secretion of 72 kDa type IV collagenase/gelatinase by cultured human lipocytes. Analysis of gene expression, protein synthesis and proteinase activity. Biochem. J. 287, 701–707.

Canbay, A., Higuchi, H., Bronk, S.F., Taniai, M., Sebo, T.J., Gores, G.J., 2002. Fas enhances fibrogenesis in the bile duct ligated mouse: a link between apoptosis and fibrosis. Gastroenterology 123, 1323–1330.

Chang, K.T., Tsai, M.J., Cheng, Y.T., Chen, J.J., Hsia, R.H., Lo, Y.S., Ma, Y.R., Weng, C.F., 2009. Comparative atomic force and scanning electron microscopy: an investigation of structural differentiation of hepatic stellate cells. J. Struct. Biol. 167, 200–208.

Chen, C.H., Yang, S.W., Shen, Y.C., 1995. New steroid acids from *Antrodia cinnamomea*, a fungal parasite of *Cinnamomum micranthum*. J. Nat. Prod. 58, 1655–1661.

Chen, J.J., Lin, W.J., Liao, C.H., Shieh, P.C., 2007. Anti-inflammatory benzenoids from *Antrodia camphorata*. J. Nat. Prod. 70, 989–992.

Chen, B.Y., Qu, P., Tie, R., Zhu, M.Z., Zhu, X.X., Yu, J., 2010. Protecting effects of vasonatrin peptide against carbon tetrachloride-induced liver fibrosis. Regul. Pept. 164, 139–143.

Chiang, H.C., Wu, D.P., Cheng, I.W., Ueng, C.H., 1995. A sesquiterpene lactone, phenyl and biphenyl compounds from *Antrodia cinnamommea*. Phytochemistry 39, 613–616.

Elsharkawy, A.M., Oakley, F., Mann, D.A., 2005. The role and regulation of hepatic stellate cell apoptosis in reversal of liver fibrosis. Apoptosis 10, 927–939.

Fan, S., Weng, C.F., 2005. Co-administration of cyclosporine an alleviates thioacetamide-induced liver injury. World J. Gastroenterol. 11, 1411–1429.

Friedman, S.L., Roll, F.J., Boyles, J., Bissell, D.M., 1985. Hepatic lipocytes: the principal collagen-producing cells of normal rat liver. Proc. Natl. Acad. Sci. USA 82, 8681–8685.

Galle, P.R., Hofmann, W.J., Walczak, H., Schaller, H., Otto, G., Stremmel, W., Krammer, P.H., Runkel, L., 1995. Involvement of the CD95 (APO-1/Fas) receptor and ligand in liver damage. J. Exp. Med. 182, 1223–1230.

Geethangili, M., Tzeng, Y.M., 2011. Review of pharmacological effects of *Antrodia camphorata* and its bioactive compounds. Evid. Based Compl. Alternat. Med. 2011, 212641.

Gressner, A.M., Weiskirchen, R., 2006. Modern pathogenetic concepts of liver fibrosis suggest stellate cells and TGF-beta as major players and therapeutic targets. J. Cell Mol. Med. 10, 76–99.

Hseu, Y.C., Chang, W.C., Hseu, Y.T., Lee, C.Y., Yech, Y.J., Chen, P.C., Chen, J.Y., Yang, H.L., 2007. Protection of oxidative damage by aqueous extract from *Antrodia camphorata* mycelia in normal human erythrocytes. Life Sci. 71, 469–482.

Hsiao, G., Shen, M.Y., Lin, K.H., Lan, M.H., Wu, L.Y., Chou, D.S., Lin, C.H., Su, C.H., Sheu, J.R., 2003. Antioxidative and hepatoprotective effects of *Antrodia camphorata* extract. J. Agric. Food Chem. 51, 3302–3308.

Huang, Y., Lu, M.Q., Li, H., Xu, C., Yi, S.H., Chen, G.H., 2006. Occurrence of cGMP/nitric oxide-sensitive store-operated calcium entry in fibroblasts and its effect on matrix metalloproteinase secretion. World J. Gastroenterol. 12, 5483–5489.

Iyer, S.S., Kusner, D.J., 1999. Association of phospholipase D activity with the detergent-insoluble cytoskeleton of U937 promonocytic leukocytes. J. Biol. Chem. 274, 2350–2359.

Kähler, C.M., Schratzberger, P., Wiedermann, C.J., 1997. Response of vascular smooth muscle cells to the neuropeptide secretoneurin. A functional role for migration and proliferation *in vitro*. Arterioscler. Thromb. Vasc. Biol. 17, 2029–2035.

Kam, Y., Exton, J.H., 2001. Phospholipase D activity is required for actin stress fiber formation in fibroblasts. Mol. Cell Biol. 21, 4055–4066.

Kawada, N., Kristensen, D.B., Asahina, K., Nakatani, K., Minamiyama, Y., Seki, S., Yoshizato, K., 2001. Characterization of a stellate cell activation-associated protein (STAP) with peroxidase activity found in rat hepatic stellate cells. J. Biol. Chem. 276, 25318–25323.

Kitamura, K., Nakamoto, Y., Akiyama, M., Fujii, C., Kondo, T., Kobayashi, K., Kaneko, S., Mukaida, N., 2002. Pathogenic roles of tumor necrosis factor receptor p55-mediated signals in dimethylnitrosamine-induced murine liver fibrosis. Lab. Invest. 82, 571–583.

Kluwe, J., Wongsiriroj, N., Troeger, J.S., Gwak, G.Y., Dapito, D.H., Pradere, J.P., Jiang, H., Siddiqi, M., Piantedosi, R., O'Byrne, S.M., Blaner, W.S., Schwabe, R.F., 2011. Absence of hepatic stellate cell retinoid lipid droplets does not enhance hepatic fibrosis but decreases hepatic carcinogenesis. Gut. 60, 1260–1268.

Kudlow, B.A., Stanfel, M.N., Burtner, C.R., Johnston, E.D., Kennedy, B.K., 2008. Suppression of proliferative defects associated with processing-defective lamin A mutants by hTERT or inactivation of p53. Mol. Biol. Cell 19, 5238–5248.

Kühn, U., Nemeth, A., Meyer, S., Wahle, E., 2003. The RNA binding domains of the nuclear poly(A)-binding protein. J. Biol. Chem. 278, 16916–16925.

Lee, U.E., Friedman, S.L., 2011. Mechanisms of hepatic fibrogenesis. Best Pract. Res. Clin. Gastroenterol. 25 (2), 195–206.

Lee, I.H., Huang, R.L., Chen, C.T., Chen, H.C., Hsu, W.C., Lu, M.K., 2002. *Antrodia camphorata* polysaccharides exhibit anti-hepatitis B virus effects. FEMS Microbiol. Lett. 209, 63–67.

Lee, T.F., Mak, K.M., Rackovsky, O., Lin, Y.L., Kwong, A.J., Loke, J.C., Friedman, S.L., 2010. Downregulation of hepatic stellate cell activation by retinol and palmitate mediated by adipose differentiation-related protein (ADRP). J. Cell Physiol. 223, 648–657.

Lee, C.C., Yang, H.L., Way, T.D., Kumar, K.J., Juan, Y.C., Cho, H.J., Lin, K.Y., Hsu, L.S., Chen, S.C., Hseu, Y.C., 2012. Inhibition of cell growth and induction of apoptosis by *Antrodia camphorata* in HER-2/neu – overexpressing breast cancer cells through the induction of ROS, depletion of HER-2/neu, and disruption of the PI3K/Akt signaling pathway. Evid. Based Compl. Alternat. Med., 17. Article ID 702857.

Lehmann, A.R., Walicka, M., Griffiths, D.J., Murray, J.M., Watts, F.Z., McCready, S., Carr, A.M., 1995. The rad18 gene of *Schizosaccharomyces pombe* defines a new subgroup of the SMC superfamily involved in DNA repair. Mol. Cell Biol. 15, 7067–7080.

Li, J., Fan, R., Zhao, S., Liu, L., Guo, S., Wu, N., Zhang, W., Chen, P., 2011. Reactive oxygen species released from hypoxic hepatocytes regulates MMP-2 expression in hepatic stellate cells. Int. J. Mol. Sci. 12, 2434–2447.

Liau, Y.J., Shaw, J.F., Lin, C.T., 2007. A highly stable cambialistic -superoxide dismutase from *Antrodia camphorata*: expression in yeast and enzyme properties. J. Biotechnol. 131, 84–91.

Liu, D.Z., Liang, H.J., Chen, C.H., Su, C.H., Lee, T.H., Huang, C.T., Hou, W.C., Lin, S.Y., Zhong, W.B., Lin, P.J., Hung, L.F., Liang, Y.C., 2007a. Comparative anti-inflammatory characterization of wild fruiting body, liquid-state fermentation, and solid-state culture of *Taiwanofungus camphoratus* in microglia and the mechanism of its action. J. Ethnopharmacol. 113, 45–53.

Liu, D.Z., Liang, Y.C., Lin, S.Y., Lin, Y.S., Wu, W.C., Hou, W.C., Su, C.H., 2007b. Antihypertensive activities of a solid-state culture of *Taiwanofungus camphoratus* (Chang-Chih) in spontaneously hypertensive rats. Biosci. Biotechnol. Biochem. 71, 23–30.

Losada, A., Hirano, T., 2005. Dynamic molecular linkers of the genome: the first decade of SMC proteins. Genes Dev. 19, 1269–1287.

Lu, J., Qin, J.Z., Chen, P., Chen, X., Zhang, Y.Z., Zhao, S.J., 2012. Quality difference study of six varieties of *Ganoderma lucidum* with different origins. Front. Pharmacol. 9 (3), 57, doi: 10.3389/fphar.2012.00057. eCollection 2012.

Lull, C., Wichers, H.J., Savelkoul, H.F., 2005. Antiinflammatory and immunomodulating properties of fungal metabolites. Mediators Inflamm. 2005, 63–80.

Maher, J.J., 2001. Interactions between hepatic stellate cells and the immune system. Semin. Liver Dis. 21, 417–426.

Muller, A., Machnik, F., Zimmermann, T., Schubert, H., 1998. Thioacetamide-induced cirrhosis-like liver lesions in rats-usefulness and reliability of this animal model. Exp. Pathol. 34, 229–236.

Nakatani, K., Okuyama, H., Shimahara, Y., Saeki, S., Kim, D.H., Nakajima, Y., Seki, S., Kawada, N., Yoshizato, K., 2004. Cytoglobin/STAP, its unique localization in splanchnic fibroblast-like cells and function in organ fibrogenesis. Lab. Invest. 84, 91–101.

Niki, T., De Bleser, P.J., Xu, G., Van Den Berg, K., Wisse, E., Geerts, A., 1996. Comparison of glial fibrillary acidic protein and desmin staining in normal and CCl_4-induced fibrotic rat livers. Hepatology 23, 1538–1545.

Ogasawara, J., Watanabe-Fukunaga, R., Adachi, M., Matsuzawa, A., Kasugai, T., Kitamura, Y., Itoh, N., Suda, T., Nagata, S., 1993. Lethal effect of the anti-Fas antibody in mice. Nature 364, 806–809.

Ozeki, T., Funakoshi, K., Iwaki, K., 1985. Rapid induction of cirrhosis by administration of carbon tetrachloride plus phospholipase D. Br. J. Exp. Pathol. 66, 385–390.

Prosser, C.C., Yen, R.D., Wu, J., 2006. Molecular therapy for hepatic injury and fibrosis: where are we? World. J. Gastroenterol. 12, 509–515.

Ramadori, G., Veit, T., Schwögler, S., Dienes, H.P., Knittel, T., Rieder, H., Meyer zum Büschenfelde, K.H., 1990. Expression of the gene of the alpha-smooth muscle-actin isoform in rat liver and in rat fat-storing (ITO) cells. Virchows Arch. B Cell Pathol. Incl. Mol. Pathol. 59, 349–357.

She, H., Xiong, S., Hazra, S., Tsukamoto, H., 2005. Adipogenic transcriptional regulation of hepatic stellate cells. J. Biol. Chem. 280, 4959–4967.

Shen, Y.C., Wang, Y.H., Chou, Y.C., Chen, C.F., Lin, L.C., Chang, T.T., Tien, J.H., Chou, C.J., 2004a. Evaluation of the anti-inflammatory activity of zhankuic acids isolated from the fruiting bodies of *Antrodia camphorata*. Planta Med. 70, 310–314.

Shen, Y.C., Chou, C.J., Wang, Y.H., Chen, C.F., Chou, Y.C., Lu, M.K., 2004b. Anti-inflammatory activity of the extracts from mycelia of *Antrodia camphorata* cultured with water-soluble fractions from five different Cinnamomum species. FEMS Microbiol. Lett. 231, 137–143.

Shim, S.G., Jun, D.W., Kim, E.K., Saeed, W.K., Lee, K.N., Lee, H.L., Lee, O.Y., Choi, H.S., Yoon, B.C., 2013. Caffeine attenuates liver fibrosis via defective adhesion of hepatic stellate cells in cirrhotic model. J. Gastroenterol. Hepatol. 28, 1877–1884.

Song, T.Y., Yen, G.C., 2002. Antioxidant properties of *Antrodia camphorata* in submerged culture. J. Agric. Food Chem. 50, 3322–3327.

Song, T.Y., Yen, G.C., 2003. Protective effects of fermented filtrate from *Antrodia camphorata* in submerged culture against CCl_4-induced hepatic toxicity in rats. J. Agric. Food Chem. 51, 1571–1577.

Sudo, K., Yamada, Y., Moriwaki, H., Saito, K., Seishima, M., 2005. Lack of tumor necrosis factor receptor type 1 inhibits liver fibrosis induced by carbon tetrachloride in mice. Cytokine 29, 236–244.

Sun, K., Wang, Q., Huang, X.H., 2006. PPAR gamma inhibits growth of rat hepatic stellate cells and TGF beta-induced connective tissue growth factor expression. Acta Pharmacol. Sin. 27, 715–723.

Szuster-Ciesielska, A., Plewka, K., Daniluk, J., Kandefer-Szerszen, M., 2011. Betulin and betulinic acid attenuate ethanol-induced liver stellate cell activation by inhibiting reactive oxygen species (ROS), cytokine (TNF-alpha, TGF-beta) production and by influencing intracellular signaling. Toxicology 280, 152–163.

Taylor, E.M., Moghraby, J.S., Lees, J.H., Smit, B., Moens, P.B., Lehmann, A.R., 2001. Characterization of a novel human SMC heterodimer homologous to the *Schizosaccharomyces pombe* Rad18/Spr18 complex. Mol. Biol. Cell 12, 1583–1594.

Torok, N., Wu, J., Zern, M., Halsted, C., French, S., Friedman, S., Znah, S.S., 2005. Phagocytosis of apoptotic bodies by hepatic stellate cells occurs in *vivo* and is an important mechanism in liver fibrogenesis. Gastroenterology 129, 1110.

Wang, W., Liu, F., Chen, N., 2007. Peroxisome proliferator-activated receptor-gamma (PPAR-gamma) agonists attenuate the profibrotic response induced by TGF-beta1 in renal interstitial fibroblasts. Mediators Inflamm 7. Article ID 62641.

Wen, L., Huang, H.M., Juang, R.H., Lin, C.T., 2007. Biochemical characterization of 1-Cys peroxiredoxin from *Antrodia camphorata*. Appl. Microbiol. Biotechnol. 73, 1314–1322.

Wen, C.L., Chang, C.C., Huang, S.S., Kuo, C.L., Hsu, S.L., Deng, J.S., Huang, G.J., 2011. Anti-inflammatory effects of methanol extract of *Antrodia cinnamomea* mycelia both *in vitro* and *in vivo*. J. Ethnopharmacol. 137, 575–584.

Wu, H., Pan, C.L., Yao, Y.C., Chang, S.S., Li, S.L., Wu, T.F., 2006. Proteomic analysis of the effect of *Antrodia camphorata* extract on human lung cancer A549 cell. Proteomics 6, 826–835.

Yu, J., Wang, Y., Qian, H., Zhao, Y., Liu, B., Fu, C., 2012. Polyprenols from *Taxus chinensis* var. *mairei* prevent the development of CCl_4-induced liver fibrosis in rats. J. Ethnopharmacol. 142 (1), 151–160.

Zhang, Y.Q., Sarge, K.D., 2008. Sumoylation regulates lamin A function and is lost in lamin A mutants associated with familial cardiomyopathies. J. Cell. Biol. 182, 35–39.